Organic & Biomolecular Chemistry

Accepted Manuscript

ROYAL SOCIETY OF CHEMISTRY

www.rsc.org/obc

Organic & Biomolecular Chemistry

RSCPublishing

PAPER

Naphthalene Diimides as Red Fluorescent pH Sensors for Functional Cells Imaging.

Cite this: DOI: 10.1039/xoxxoooooox

Received ooth January 2012,
Accepted ooth January 2012

DOI: 10.1039/xoxxoooooox

www.rsc.org/

Filippo Doria,*[a] Marco Folini,[b] Vincenzo Grande,[a] Graziella Cimino-Reale,[b] Nadia Zaffaroni[b] and Mauro Freccero.*[a]

A small library of hydrosoluble naphthalene diimides (NDIs) was designed and synthesized, as cell permeable pH "turned-on" fluorescent sensors, for cellular applications. The NDIs exhibit a non-emitting twisted intramolecular charge transfer (TICT) state, which has been described by a DFT computational investigation. These NDIs do not emit as free-base, but they become strong emitters when protonated. Switching of the red emission was achieved in the pH window 2.5-6, tuning steric and electronic features of the amine moiety. The least acidic protonated NDI (**5**, pK_a 5.1) was investigated in normal and cancer cells. Its selective redistribution in cancer cell from acidic vesicular organelles to the cytoplasm and the nucleus, describes an effective application of these NDIs as valuable functional tool.

Introduction

Intracellular pH (pHi) represents one of the most important cell homeostasis regulators and it plays a key role in numerous metabolic pathways. These physiological events require a stringent regulation of pH values that has to be maintained in the range of 6.8-7.4.[1-5] Abnormal pHi values are often associated with inappropriate cell function, growth and division. In particular, it is well known how acidosis is strictly correlated with tumour microenvironment, cell apoptosis and autophagy process.[6-13] In this context, H_3O^+ has became one of the most important targets among intracellular species.[14] Recently, small fluorescent organic molecules have been widely studied as pH probes.[15-23] Among many methods for cellular pH measurement, fluorescence microscopy had become one of the most powerful tools, thanks to its high spatial and temporal resolution. Nonetheless, the current challenge is to design a probe with proper cellular permeability that should be able to detect pH in a weakly acidic environment. Consequently, the development of ratiometric and intracellular pH sensors is highly desirable. With this goal in mind, we designed a family of naphthalene diimides (NDIs) as membrane-permeable probes of high sensitivity towards pHi micro-modifications. The NDI dyes are widely used sensors in organic media thanks to their high fluorescence quantum yield, absorption and emission spectra, which can be easily tuned in the visible region from green to red and near-IR.[24-34] The latter are particularly welcome for bio-applications as the signal can penetrate tissues, improve detection and erase any potential photo-damage. Previously, we investigated different classes of hydrosoluble naphthalene diimides with promising photophysical properties that led us to design new pH probes based on NDI core.[35-39] Herein, we reported a new class of "turn on" core-substituted cNDIs with a tertiary nitrogen atom directly bound to the aromatic core, which exhibit pH dependent susceptibility (**1-5**, Scheme 1).

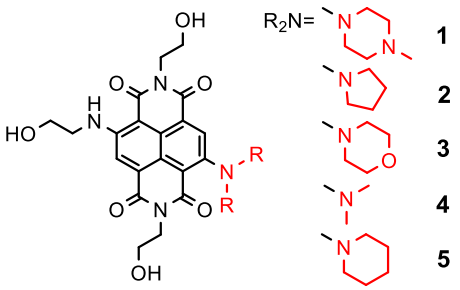

Scheme 1. Naphthalene diimides (NDIs, **1-5**) synthesized and investigated as pH sensors. The red moieties control the emission properties.

Moreover, we explored several aromatic tertiary amines as substituents on the NDI core, in order to fine-tune the *pKa* of the conjugate acid.

Results and discussion

The NDI derivatives here proposed were obtained following the synthesis shown in Scheme 2. The 2,6-dibromo-1,4,5,8-naphthalenetetracarboxylic dianhydride was easily prepared

according to a reported procedure, starting from the commercially available anhydride.[40-42]

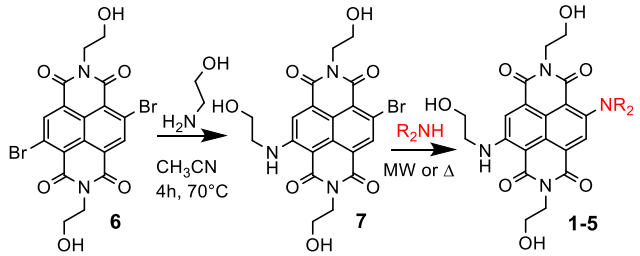

Scheme 2. Synthesis of the NDIs **1-5**.

The first step, in Scheme 2, is an imidation reaction under acidic conditions, yielding the 2,6-dibromo-substituted NDI **6**. The subsequent nucleophilic aromatic substitution (S_NAr) on **6** by ethanolamine, according to a mild optimized protocol (CH_3CN as solvent, 70°C, 4h), afforded **7** in good yield. The S_NAr under these conditions was selective, yielding only the mono Br-functionalized product, which was readily used for an additional S_NAr. The final step, was performed dissolving **7** in neat secondary amines, under both mild (50°C, 2h), and microwave assisted (180 °C, 200 psi, 200 W, 3 min) conditions, to give the NDIs **1-5** in good yields. The microwave-assisted protocol systematically give rise to almost quantitative yields (Supp. Inf., for procedure details).

The NDIs **1-5** are non-fluorescent under neutral or basic conditions ("off" state). On the contrary, the conjugate acids **1H-5H**, which are populated under mild acidic conditions, exhibit an intense red emission ("on" state). Furthermore, upon the addition of an acid, the NDI dyes change colour from blue to red. In order to characterise the optical properties of these potentially useful pH sensors, fluorescence and absorption titrations, were carried out for all the NDI synthesized. Both the above techniques were consistent to suggest the *pKa* values summarised in Table 1.

The effect of the different amino moieties on the NDIs **1-5** basicity is remarkable, as the pK_a values of their conjugate acids (**1H-5H**) span from 0.5 to 5.1 (Table 1). NDI **5** has been chosen as exemplificative model, as its highest *pKa* value (5.1) offers interesting opportunity for in vivo applications. Nevertheless, similar titrations have been recorded for the NDIs **1-4** (Supp. Inf.). Indeed, the free base absorption was comparable to classical core bis-substituted NDIs with a band above 600 nm (608 nm, pH = 9), as shown in Figure 1a. Progressively more acidic conditions induced a gradual decrease of this band and the appearance of a new blue-shifted band centred at 530 nm (pH = 2.3), which is very similar to that exhibited by several core mono-substituted NDIs.[37] The bright NDI **5H** showed a strong fluorescence emission at 613 nm, with a good quantum yield (Φ_F=0.22). Similar behaviour was recorded for **3H-4H** under acid conditions (pH 2.0, phosphate buffer). The NDIs **1H** and **2H** were much less fluorescent under identical acid conditions.

Table 1. Photophysical and chemical properties of the NDI sensors.

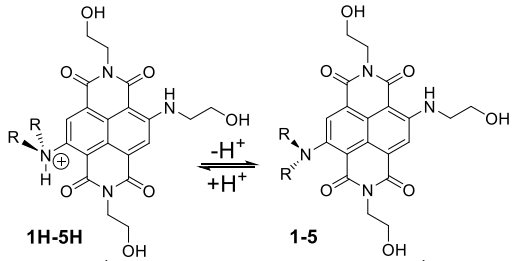

NDIs[a]	λ_{max}/nm[b]	$\varepsilon_{max}/10^{-3}M^{-1}cm^{-1}$ [c]	λ_{em}/nm[d]	Φ_F[e]	*pKa*
1H	546	9.4	634	0.05	0.5
2H	536	5.72	610	0.07	2.4
3H	556	2.07	618	0.22	2.6
4H	533	7.13	608	0.23	4.2
5H	530	3.45	613	0.22	5.1

[a] Conjugate acids (**1H-5H**) of the NDI dyes (**1-5**). [b] Wavelength of maximum absorption measured in acid aqueous solution by HNO_3 (pH 2.0). [c] Molar absorptivity, in acid phosphate buffer (pH 2.0). [d] Emission wavelength. [e] Fluorescence quantum yields, measured in acid in acid phosphate buffer (pH 2.0), relative to the reference NDI **8** (see Supporting information for structure detail).[37]

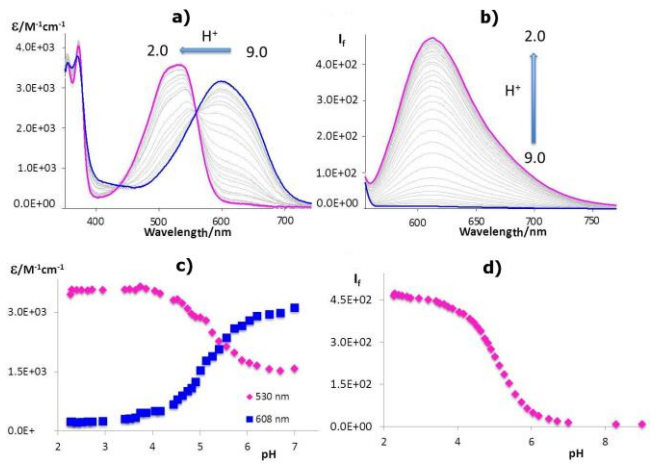

Figure 1. a) Absorption and b) Fluorescence spectra of **5** upon pH titration. c) pH-dependent absorption at 530 and 608 nm, yielding a *pKa* value of 5.1. d) "Turned-on" of the emission of **5** at 613 nm as function of the pH.

The lack of fluorescence of the weak bases **1-5** may be a result of a non-emitting twisted intramolecular charge transfer (TICT) state. In fact, the emission of the NDI core should be switched off by electron transfer (eT) from an electronically isolated amino moiety, which is not planar neither in the ground state nor in the singlet excited state (Figure 2). On the contrary, the protonated ammonium moieties in the NDIs **1H-5H**, cannot longer quench the fluorophore by eT, resulting into an intense red emission.

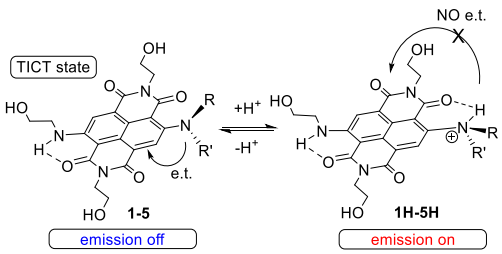

Figure 2. Protonation of the tertiary amine moiety suppresses the TICT state of the NDIs **1-5**, turning on the emission.

To support the hypothesis of a non-emitting twisted intramolecular charge transfer (TICT) state for the NDIs **1-5**, calculations were carried out in the frame of density functional theory (DFT) and time-dependent density functional theory (TDDFT) at the B3LYP/6-31+G(d,p) level using Gaussian 09 software. The geometry optimization of ground state (S_o) and first singlet excited state (S_1) of **4**, used as a model (Figure 3a and 3b, respectively), suggest for both a non-planar amino moiety to the aromatic NDI core. The deviation from planarity is moderate for S_o (θ = $C_1C_2N_1C_3$, 21.3°), but becomes remarkable for the S_1 (θ =83.6°), with improved charge transfer from the amino moiety to the NDI core (Supp. Inf). Such a resulting TICT state involving a free amino rotor is not an emitting state. The protonation induce a sharp structural change, erasing the donor properties of the resulting ammonium moiety, which behaves as locked rotor with a θ =64° in both S_o and S_1 states, due to a very strong intramolecular H-bonding, involving the proximal carbonyl oxygen of the amide functional group (Figures 3c and 3d). Remarkably, the torsion of the ammonium moiety becomes even more hindered in the S_1 state of **4H**, as the latter exhibits a stronger intramolecular H-bonding than in the S_0, with a shorter NH···O intramolecular H-bonding (Figures 3d *vs* 3c).

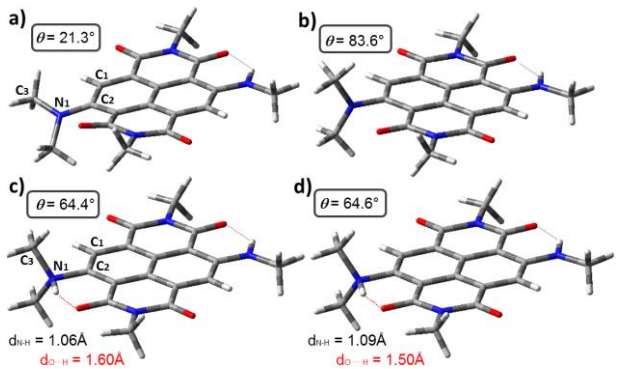

Figure 3. B3LYP/6-31G(d,p) and TD-B3LYP/6-31G(d,p) gas phase optimised geometries of a): the ground state (S_o), b) first singlet excited state (S_1) of **4,** c) S_o and d) S_1 of the conjugate acid **4H**. The torsional dihedral angle θ($C_1C_2N_1C_3$) values and the NH and H-bonding O···H distances are reported.

The emission properties described above, together with a pK_a value 5.1, clearly suggest the NDI **5** is a lead sensor for *in-cellulo* applications. To evaluate the selectivity of our sensor toward the proton, we measured the fluorescence emission spectra of both **4** and **5** in the presence of metal ions (Na^+, K^+, Ca^{2+}, Mg^{2+}, Zn^{2+}, Mn^{2+}, Cu^{2+}, Fe^{2+}, Fe^{3+}) or other biological relevant species (e.g., glutathione, Cys, Gly, Tyr and Vit C) under buffered conditions (pH = 6.0, 25°C). As expected, these species caused no effect on the emission, indicating that NDI **5** could be used for pHi measurements without any potential interference by biological relevant species. In order to examine the potential applicability in living cells of our sensor, cell-imaging studies were performed using the commercially available prostate cancer (PC-3) cell line. Fluorescence microscopy analysis showed that NDI-**5** was efficiently taken up by PC-3 cells incubated at 37 °C for 90 min in the presence of 60 µmol L^{-1} of the compound (Figure 4A). Specifically, the compound distributed throughout the cytoplasm in intracellular vesicular structures as suggested by the typical dotted pattern of the red fluorescence signal originated by NDI-**5**. This observation indicates that **5** was likely taken up by cells *via* endocytosis and resided within acidic vesicular organelles (e.g., late endosome/lysosomes).[43] Such a hypothesis gains support by *i)* the observation that no red fluorescence signal was appreciable in PC-3 cells exposed to the same drug concentration and incubated for 90 min at 4°C (Figure 4B) and *ii)* the finding that **5** co-localized with lysosomes in PC-3 cells as revealed by the evidence that the punctuate red fluorescence signal generated by the compound matched, at least in part, that of LAMP-2A, a specific lysosome membrane marker, probed with an AlexaFluor®488-labelled secondary antibody (Figure 4C).

An unifying feature of solid tumors is a markedly altered pH compared to normal tissues, due to i) a metabolic shift toward acid-producing pathways (i.e., Warburg effect); ii) the poorly perfused tumor microenvironment, resulting in a reduced diffusive flux of acid equivalents and iii) an altered expression levels of pH-regulatory proteins.[44] It is widely recognized that the alkalinisation of pHi of cancer cells is accompanied by the acidification of the extracellular environment. This phenomenon is considered to directly drive the metastatic process and to contribute to the multidrug resistance phenotype.[45] In addition, the accumulation of intracellular acidity is an early event responsible for the activation and execution of the apoptotic program (i.e., programmed cell death).[46] As a consequence, in order to survive cancer cells devised a variety of detoxification mechanisms to counteract any drop in the pHi.[46] Specifically, the regulation of pH in cancer cells are primarily achieved by proton pumps which, through various mechanisms, have the net effect of externalising protons, ultimately leading to a drop in the pH of the extracellular space and a concomitant increase in the pHi.[45] Vacuolar type H^+-ATPases (V-ATPases) have been identified as the main mediators of pH regulation in tumors. They are expressed in the plasma membrane as well as in membranes of intracellular organelles (i.e., lysosomes, endosomes) resulting in their acidification. The up-regulation of V-ATPases is an event frequently observed in most human tumor cells. This evidence, together with the fundamental role in the regulation of pHi, suggests

that these pumps might represent viable therapeutic targets in cancer.[46] Indeed, several V-ATPase inhibitors have been described,[45] among which the most studied and thoroughly used are macrolide antibiotics, namely, bafilomycins and concanamycins.[45] These agents used at nanomolar concentrations selectively inhibit V-ATPase, resulting in cell growth inhibition and apoptosis induction in different human cancer cells.[45] Interestingly, proton pump inhibition results in the acidification of pHi, an event that can be exploited to achieve tumor-specific uptake or activation of certain agents the effect of which are pH-dependent.[47]

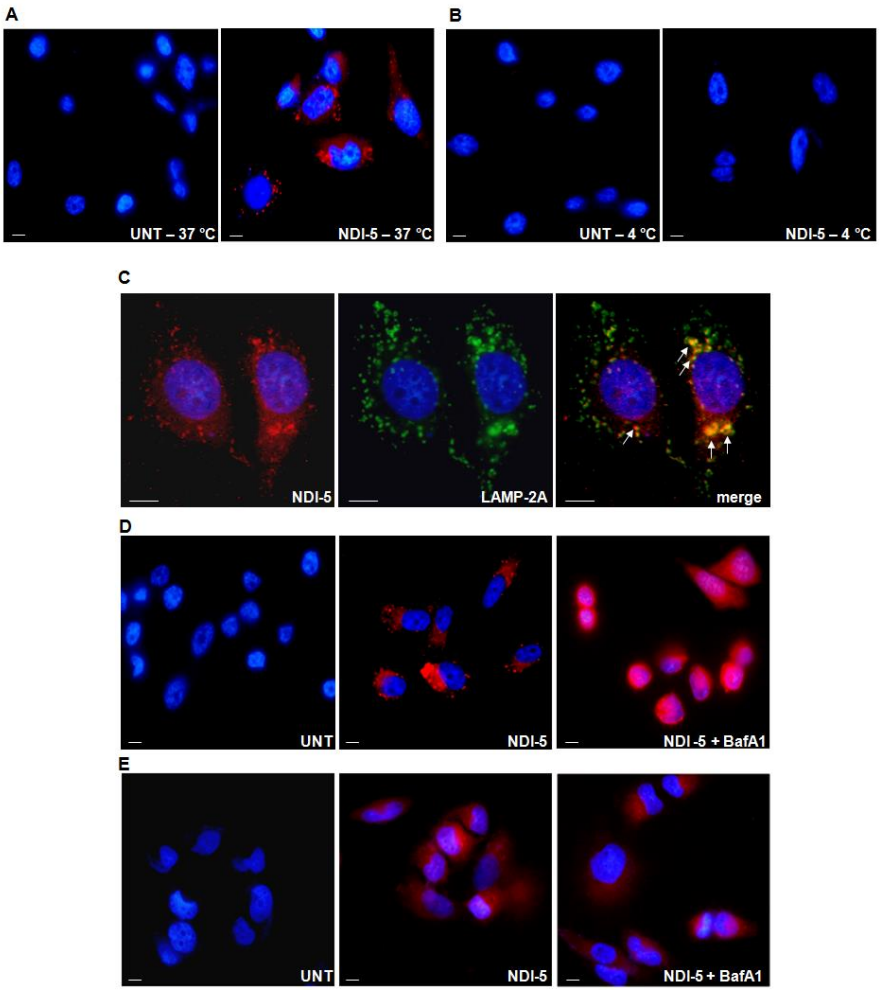

Figure 4: Cell imaging studies of the internalization of NDI-**5** in prostate cells. (**A**, **B**) Representative images showing the internalization of **5** assessed by fluorescence microscopy (red signal, Tetramethylrhodamine isothiocyanate filter) on PC-3 cells grown on glass coverslips, exposed to 60 µmol L^{-1} of the compound and incubated for 90 min at 37 °C or 4 °C. (**C**) NDI-**5** is retained within acidic vesicular organelles, as suggested by the typical dotted fluorescent pattern. It partially localized with lysosomes, as shown by the match between the distribution pattern of its fluorescence signal (*left panel*) and that of LAMP-2A (*middle panel*). White arrows in *right panel* indicate the co-localization of **5** (red) and LAMP-2A (green). (**D**) The capability of **5** to sense changes in the pHi was investigated in PC-3 cells treated for 3 h with 50 nmol L^{-1} of BafA1 (a non toxic concentration identified by preliminary experiments, data not shown). A marked increase in the intensity of the red fluorescence signal originated by **5**, paralleled by the redistribution of the compound throughout the cytoplasm and the nucleus, was clearly appreciable in BafA1-treated PC-3 cells compared to cells exposed to **5** alone. (**E**) Such an effect was specific for cancer cells, as no changes in the fluorescence intensity and distribution pattern of the pH sensor was appreciable in **5**-treated PTNA1 cells, irrespective of exposure to BafA1. UNT: untreated cells. Nuclei were counterstained with 4',6-diamidino-2-phenylindole (DAPI). Magnifications ×40 (panels A,B,D,E) and ×60 (panel C). Scale bars: 10 µm.

In this context, the capability of our NDI derivative to sense any drop in the pHi was investigated in PC-3 cells exposed to **5** and subsequently treated with Bafilomycin A1 (BafA1). Cell imaging analysis showed that the inhibition of V-ATPases by BafA1 induced an increase in the intensity of the red fluorescence signal originated by **5**, which concomitantly redistributed within the cytoplasm and the nucleus of PC-3 cells compared to the typical punctuate fluorescent pattern of the compound observed in cells that were not exposed to BafA1 (Figure 4D). This evidence corroborates our hypothesis of the endocytic sequestration of the drug within cancer cells. In fact, the diffused pattern of **5** fluorescent signal observed in the presence of BafA1 is indicative of an endosome/lysosome escape of the drug.[43] Moreover, our findings suggest that **5** is actually a good pH sensor in cancer cells as the marked increase in the intensity of the fluorescence signal paralleled the

acidification of pHi consequent to the inhibition of V-ATPases. In addition, no changes in the fluorescence emission and intracellular distribution of the pH sensor was observed in the normal prostate epithelial PTNA1 cells exposed to both **5** and BafA1 compared to cells treated with only **5** (Figure 4E). This observation deals with the notion that cancer cells have a higher pHi and overexpress V-ATPase, consequently becoming more sensitive to BafA1 treatment (i.e., drop of the pHi), compared to normal cells. [46-48]

Conclusions

Overall, our data showed that the rationally designed NDI-**5** is actually a biologically relevant pH sensor that is a useful tool for both the selective staining of acidic vesicular organelles and to sense possible changes in the pHi associated to treatment-induced cell stress or death in living cultured cells. In addition, a future possible application of similar NDI-based pH sensors, exhibiting *pKa* values closer to neutrality, to monitor the pH of the extracellular environment, may be also envisaged in order to distinguish tumor from normal tissue *in vivo*.

Experimental Section

General procedure for the microwave-assisted (MW) nucleophilic aromatic substitution. Microwave-assisted (MW) reactions were carried out with a CEM© Discover reactor. **7** (0.05 mmol) was dissolved into 2 mL of neat amine. The mixture was stirred and heated in sealed vessels, at 180°C, 200 psi, 200 W, for 3 min. The resulting blue solution was cooled at r.t. and purified by preparative HPLC chromatography, using a C-18 reversed-phase column (CH_3CN/H_2O 0.1% TFA, preparative method). HCl 1 M solution was added to each chromatographic portion. Solvent evaporation under vacuum afforded the adducts **1** (89% yield), **2** (90% yield), **3** (88% yield) and **5** (95% yield).

General procedure for the nucleophilic aromatic substitution at 50°C. 7 (0.05 mmol) was dissolved into 2 mL of neat amine. The mixture was stirred and heated at 50°C, for 2 h. The resulting violet solution was cooled at r.t., and purified by preparative HPLC chromatography, using a C-18 reversed-phase column (CH_3CN/H_2O 0.1% TFA, preparative method), HCl 1 M solution was added to each chromatographic portion. Solvent evaporation under vacuum afforded the adducts **1** (71% yield), **2** (67% yield), **3** (59% yield) and **5** (73% yield).

N,N'-Bis-(hydroxyethyl)-2-(N'-methyl-N-piperazinyl)-6-(hydroxyethylamino)-1,4,5,8-tetracarboxylic acid bisimide hydrochloride (1·2HCl): Dark pink solid. M.p. dec. >200°C; ^{1}H NMR (300 MHz, D_2O-DCl): δ (ppm) =8.37 (s, 1H); 8.00 (s, 1H); 3.98 (m, 2H); 3.84 (m, 6H); 3.70 (m, 2H); 3.54 (m, 2H); 3.41 (m, 8H); 2.71 (s, 3H); ^{13}C NMR (75 MHz, D_2O-DCl): δ (ppm) =165.4; 164.5; 161.8; 161.3; 151.9; 145.6; 134.0; 128.7; 125.7; 123.6; 123.3; 119.2; 115.1; 98.0; 59.0; 57.7; 57.4; 50.7; 50.0; 43.2; 41.3; 40.5. Anal. Calcd. for $C_{25}H_{31}Cl_2N_5O_7$: C, 51.38; H, 5.35; N, 11.98. Found: C, 51.57; H, 5.32; N, 11.93.

N,N'-Bis-(hydroxyethyl)-2-(N-pirrodinyl)-6-(hydroxyethylamino)-1,4,5,8-tetracarboxylic acid bisimide hydrochloride (2·HCl): Dark pink solid. M.p. dec. >200°C; ^{1}H NMR (300 MHz, D_2O-DCl): δ (ppm) =8.72 (s, 1H); 8.46 (s, 1H); 4.31 (m, 6H); 3.90 (m, 10H); 2.58 (m, 2H); 2.41 (m, 2H); ^{13}C NMR (75 MHz, D_2O-DCl): δ (ppm) =166.6; 166.0; 163.3; 162.8; 153.1; 137.3; 129.6; 127.2; 126.1; 124.9; 124.2; 123.5; 116.9; 99.5; 60.5; 60.0; 59.2; 58.9; 44.5; 42.5; 41.8; 24.4. Anal. Calcd. for $C_{24}H_{27}ClN_4O_7$: C, 55.55; H, 5.24; N, 10.80. Found: C, 55.60; H, 5.32; N, 10.73.

N,N'-Bis-(hydroxyethyl)-2-(N-morpholinyl)-6-(hydroxyethylamino)-1,4,5,8-tetracarboxylic acid bisimide hydrochloride (3·HCl): Dark pink solid. M.p. dec. >200°C; ^{1}H NMR (300 MHz, D_2O-DCl): δ (ppm) =8.78 (s, 1H); 8.37 (s, 1H); 4.23 (m, 6H); 4.08 (m, 4H); 3.8 (m, 10H); ^{13}C NMR (75 MHz, D_2O-DCl): δ (ppm) =167.2; 166.2; 163.5; 163.0; 153.6; 136.5; 130.2; 127.4; 125.0; 124.0; 123.2; 120.5; 116.6; 99.6; 65.4; 60.7; 59.4; 59.0; 55.4; 47.9; 44.7; 42.8; 42.0. Anal. Calcd. for $C_{24}H_{27}ClN_4O_8$: C, 53.89; H, 5.09; N, 10.47. Found: C, 53.87; H, 5.12; N, 10.43.

N,N'-Bis-(hydroxyethyl)-2-(N-dimethylamino)-6-(hydroxyethylamino)-1,4,5,8-tetracarboxylic acid bisimide hydrochloride (4·HCl): 7 (0.05 mmol) was dissolved into 2 mL of a saturated solution of dimethylamine in DMF. The mixture was stirred and heated in a microwave reactor, in sealed vessels, at 180°C, 200 psi, 200 W, for 3 min. The resulting blue solution was cooled at r.t. and purified by preparative HPLC chromatography, using a C-18 reversed-phase column (CH_3CN/H_2O 0.1% TFA, preparative method). HCl 1 M solution was added and the solvent evaporation under vacuum, affording the adduct **4** (yield 57%). Dark pink solid. M.p. dec. >200°C; ^{1}H NMR (300 MHz, CD_3OD-DCl): δ (ppm) =8.89 (s, 1H); 8.52 (s, 1H); 4.38 (m, 4H); 3.89 (m, 8H); 3.62 (s, 3H); ^{13}C NMR (75 MHz, D_3OD-DCl): δ (ppm) =167.8; 163.9; 163.6; 154.6; 140.4; 131.3; 129.3; 126.6; 124.8; 124.0; 121.5; 118.2; 100.7; 61.5; 60.1; 59.8; 47.8; 46.1; 43.8; 42.9. Anal. Calcd. for $C_{22}H_{25}ClN_4O_7$: C, 53.61; H, 5.11; N, 11.37. Found: C, 53.57; H, 5.25; N, 11.31.

N,N'-Bis-(hydroxyethyl)-2-(N-piperidinyl)-6-(hydroxyethylamino)-1,4,5,8-tetracarboxylic acid bisimide hydrochloride (5·1HCl): Dark pink solid. M.P. dec. >200°C; ^{1}H NMR (300 MHz, D_2O-DCl): δ (ppm) =8.60 (s, 1H); 8.18 (s, 1H); 4.09 (m, 4H); 3.67 (m, 12H); 2.0-1.81 (m, 6H). ^{13}C NMR (75 MHz, D_2O-DCl): δ (ppm) =165.5; 164.7; 162.1; 161.7; 152.0; 136.7; 128.5; 126.0; 123.5; 123.2; 121.9; 119.0; 115.0; 98.1; 59.2; 57.8; 57.6; 56.1; 43.4; 41.5; 40.7; 23.5; 17.3. Anal. Calcd. for $C_{25}H_{29}ClN_4O_7$: C, 56.34; H, 5.48; N, 10.51. Found: C, 56.41; H, 5.42; N, 10.53.

Acknowledgements

Financial support from the Italian Ministry of Education, University and Research (MIUR), Rome (Grants: FIRB-Ideas RBID082ATK_003) and from the Italian Association for Cancer Research (AIRC, IG2013-14708) is gratefully acknowledged.

Notes and references

[a] Dipartimento di Chimica, Università di Pavia,
V.le Taramelli 10, 27100 Pavia (Italy)
E-mail: filippo.doria@unipv.it ; mauro.freccero@unipv.it
[b]Molecular Pharmacology Unit, Department of Experimental Oncology and Molecular Medicine, Fondazione IRCCS Istituto Nazionale dei Tumori, via G. Amadeo, 42 – 20133, Milano, Italy.

Electronic Supplementary Information (ESI) available: Experimental and computational details as well as spectroscopic and analytical data for new compounds. See DOI: 10.1039/b000000x/

1 W. B. Busa, *Annual Rev. Physiol.*, 1986, **48**, 389-402.
2 W. B. Busa and R. Nuccitelli, *Am. j. physiol.*, 1984, **246**, 409-438.
3 J. R. Casey, S. Grinstein and J. Orlowski, *Nat. Rev. Molec. Cell. Biol.*, 2010, **11**, 50-61.
4 M. Chesler, *Physiol. Rev.*, 2003, **83**, 1183-1221.
5 H. Izumi, T. Torigoe, H. Ishiguchi, H. Uramoto, Y. Yoshida, M. Tanabe, T. Ise, T. Murakami, T. Yoshida, M. Nomoto and K. Kohno, *Cancer Treat. Rev.*, 2003, **29**, 541-549.
6 J. Chiche, K. Ilc, J. Laferriere, E. Trottier, F. Dayan, N. M. Mazure, M. C. Brahimi-Horn and J. Pouyssegur, *Cancer Res.*, 2009, **69**, 358-368.
7 K. A. Christensen, J. T. Myers and J. A. Swanson, *J. Cell Sci.*, 2002, **115**, 599-607.
8 J. E. DiCiccio and B. E. Steinberg, *J. Gen. Physiol.*, 2011, **137**, 385-390.
9 T. Fukuda, L. Ewan, M. Bauer, R. J. Mattaliano, K. Zaal, E. Ralston, P. H. Plotz and N. Raben, *Ann. of Neurol.*, 2006, **59**, 700-708.
10 S. J. Lee, M. H. Park, H. J. Kim and J. Y. Koh, *Glia*, 2010, **58**, 1186-1196.
11 A. Rivinoja, N. Kokkonen, I. Kellokumpu and S. Kellokumpu, *J. Cell. Physiol.*, 2006, **208**, 167-174.
12 X. Zhang, Y. Lin and R. J. Gillies, *J. Nucl. Med.*, 2010, **51**, 1167-1170.
13 R. A. Cardone, V. Casavola and S. J. Reshkin, *Nat. Rev. Cancer*, 2005, **5**, 786-795.
14 J. Han and K. Burgess, *Chem. Rev.*, 2010, **110**, 2709-2728.
15 Q. A. Best, C. Liu, P. D. van Hoveln, M. E. McCarroll and C. N. Scott, *J. Org. Chem.*, 2013, **78**, 10134-10143.
16 M. F. Juette, D. S. Terry, M. R. Wasserman, Z. Zhou, R. B. Altman, Q. Zheng and S. C. Blanchard, *Curr. Opin. Chem. Biol.*, 2014, **20**, 103-111.
17 H. Lee, W. Akers, K. Bhushan, S. Bloch, G. Sudlow, R. Tang and S. Achilefu, *Bioconjug. Chem.*, 2011, **22**, 777-784.
18 G. Li, D. Zhu, L. Xue and H. Jiang, *Org. Lett.*, 2013, **15**, 5020-5023.
19 P. Li, H. Xiao, Y. Cheng, W. Zhang, F. Huang, W. Zhang, H. Wang and B. Tang, *Chem. Comm.*, 2014, **50**, 7184-7187.
20 L. J. Tauzin, B. Shuang, L. M. Kisley, A. P. Mansur, J. Chen, A. de Leon, R. C. Advincula and C. F. Landes, *Langmuir*, 2014, **30**, 8391–8399.
21 S. Wu, S. Han, J. Han and X. Su, *Chem. Comm.*, 2014, **50**, 8014-8017.
22 L. Xue, G. Li, D. Zhu, Q. Liu and H. Jiang, *Inorg. Chem.*, 2012, **51**, 10842-10849.
23 S. Yang, Y. Qi, C. Liu, Y. Wang, Y. Zhao, L. Wang, J. Li, W. Tan and R. Yang, *Anal. Chem.*, 2014, **86**, 7508–7515.
24 T. D. Bell, S. Yap, C. H. Jani, S. V. Bhosale, J. Hofkens, F. C. De Schryver, S. J. Langford and K. P. Ghiggino, *Chemistry, Asian J.*, 2009, **4**, 1542-1550.
25 S. V. Bhosale, S. V. Bhosale, M. B. Kalyankar and S. J. Langford, *Org. Lett.*, 2009, **11**, 5418-5421.
26 D. A. Doval, A. Fin, M. Takahashi-Umebayashi, H. Riezman, A. Roux, N. Sakai and S. Matile, *Org. Biomol. Chem.*, 2012, **10**, 6087-6093.
27 A. Fin, I. Petkova, D. A. Doval, N. Sakai, E. Vauthey and S. Matile, *Org. Biomol. Chem.*, 2011, **9**, 8246-8252.
28 S. Hagihara, L. Gremaud, G. Bollot, J. Mareda and S. Matile, *J. Am. Chem. Soc.*, 2008, **130**, 4347-4351.
29 H. F. Higginbotham, R. P. Cox, S. Sandanayake, B. A. Graystone, S. J. Langford and T. D. Bell, *Chem. Comm.*, 2013, **49**, 5061-5063.
30 H. Langhals and H. Jaschke, *Chem. Eur. J.*, 2006, **12**, 2815-2824.
31 Q. Li, M. Peng, H. Li, C. Zhong, L. Zhang, X. Cheng, X. Peng, Q. Wang, J. Qin and Z. Li, *Org. Lett.*, 2012, **14**, 2094-2097.
32 X. Lu, W. Zhu, Y. Xie, X. Li, Y. Gao, F. Li and H. Tian, *Chem. Eur. J.*, 2010, **16**, 8355-8364.
33 C. Zhou, Y. Li, Y. Zhao, J. Zhang, W. Yang and Y. Li, *Org. Lett.*, 2011, **13**, 292-295.
34 S. V. Bhosale, N. V. Ghule, M. Al Kobaisi, M. M. Kelson and S. V. Bhosale, *Chem. Eur. J.*, 2014, **20**, 10775 – 10781.
35 F. Doria, M. di Antonio, M. Benotti, D. Verga and M. Freccero, *J. Org. Chem.*, 2009, **74**, 8616-8625.
36 F. Doria, C. M. Gallati and M. Freccero, *Org. Biomol. Chem.*, 2013, **11**, 7838-7842.
37 F. Doria, I. Manet, V. Grande, S. Monti and M. Freccero, *J. Org. Chem.*, 2013, **78**, 8065-8073.
38 F. Doria, M. Nadai, M. Folini, M. Scalabrin, L. Germani, G. Sattin, M. Mella, M. Palumbo, N. Zaffaroni, D. Fabris, M. Freccero and S. N. Richter, *Chem. Eur. J.*, 2013, **19**, 78-81.
39 F. Doria, M. Nadai, G. Sattin, L. Pasotti, S. N. Richter and M. Freccero, *Org. Biomol. Chem.*, 2012, **10**, 3830-3840.
40 F. Doria, M. Nadai, M. Folini, M. Di Antonio, L. Germani, C. Percivalle, C. Sissi, N. Zaffaroni, S. Alcaro, A. Artese, S. N. Richter and M. Freccero, *Org. Biomol. Chem.*, 2012, **10**, 2798-2806.
41 C. Roger and F. Wurthner, *J. Org. Chem.*, 2007, **72**, 8070-8075.
42 C. Thalacker, C. Roger and F. Wurthner, *J. Org. Chem.*, 2006, **71**, 8098-8105.
43 Z. Ouar, M. Bens, C. Vignes, M. Paulais, C. Pringel, J. Fleury, F. Cluzeaud, R. Lacave and A. Vandewalle, *Biochem. J.*, 2003, **370**, 185-193.
44 A. Gorbatenko, C. W. Olesen, E. Boedtkjer and S. F. Pedersen, *Front. Physiol.*, 2014, **5**, 130.
45 M. Perez-Sayans, J. M. Somoza-Martin, F. Barros-Angueira, J. M. Rey and A. Garcia-Garcia, *Cancer Treat. Rev.*, 2009, **35**, 707-713.
46 C. Daniel, C. Bell, C. Burton, S. Harguindey, S. J. Reshkin and C. Rauch, *Biochim. Biophys. Acta*, 2013, **1832**, 606-617.
47 M. F. McCarty and J. Whitaker, *Altern. Med. Rev.*, 2010, **15**, 264-272.
48 M. Damaghi, J. W. Wojtkowiak and R. J. Gillies, *Front. Physiol.*, 2013, **4**, 370.

